Scanning Electron Microscopy

Volume 1985
Number 2 *Part II*

Article 2

6-15-1985

# Approach to a Stable Field Emission Electron Source

H. Adachi
*Oregon Graduate Center*

SCANNING ELECTRON MICROSCOPY/1985/II (Pages 473-487)
SEM Inc., AMF O'Hare (Chicago), IL 60666 USA

0586-5581/85$1.00+.05

# APPROACH TO A STABLE FIELD EMISSION ELECTRON SOURCE

H. Adachi*

(Visiting Scientist)
Oregon Graduate Center
19600 N.W. Von Neumann Drive
Beaverton, Oregon 97006-1999

Phone no: (503) 645-1121

(Paper received February 26 1985, Completed manuscript received June 15 1985)

## Abstract

Field emission occurs at the sharp apex of a metal needle, so that it can be considered as providing a point electron source, which is a desirable feature for a fine focused electron beam. The disadvantage is its low stability. It is shown that the current fluctuations occur mainly due to the interaction with the residual gas in the vacuum; thus reduction of the interaction with the residual gas is essential for a stable field electron source. The stringency of the vacuum requirement has prevented wide application of the field emission electron source. New materials which have low work functions and high melting points are examined in the view of a stable field electron emitter, and it is shown that carbides of transition metals have potential as a stable field emitter. Very stable field emission has been reported for TiC single crystals. Operation in the thermal-field emission mode is examined and it is shown that ZrO/W(100) emitter gives stable emission, whose fluctuation is less than 0.23% in the frequency interval 1 to 5000 Hz. The only disadvantage of the ZrO/W thermal field emitter is its rather high level of instability at very low frequencies. This paper reviews the development of field electron emission as it is applied to electron sources.

Key Words: Electron gun, Cathode, TiC, TaC, ZrO/W, Field emission, Cold Field emission, Thermal field emission, High brightness.

* On leave from: Department of Applied Materials Science, Muroran Institute of Technology, 27-1 Mizumoto-cho, Muroran, 050 JAPAN Phone no.: 143-44-4181

## Introduction

Field emission electron sources have superior characteristics of small source size, of high brightness and of narrow energy spread for production of fine focused electron beams [14, 15,16,18,21,57,87]. They have been successfully applied to many micro electron probes, such as high resolution scanning electron microscopes (SEM) [13,20,21,45,50,64,70,88], conventional transmission microscopes (CTEM) [15,37,67,81,85], scanning transmission microscopes (STEM) [8,13, 19,46,69,89], scanning Auger microscopes (SAM) [82], microbeam testing devices for very large scale integrated circuits (VLSI) [77], electron beam lithography systems [26,44,68], etc.. They also have an advantage in the production of low energy fine focused electron beams [53,77,83].

The electron current passing through an area is proportional both to the area and to the solid angle subtended by any field illuminating aperture at the source. The constant of proportionality is known as the beam brightness, which is approximately proportional to accelerating voltage. The brightness of the field emitter is measured to be about $2 \times 10^8$ A/sr cm$^2$ some 2-3 orders of magnitude greater than that of the thermionic cathode [52]. The brightness of the thermionic $LaB_6$ cathode lies in the range $5 \times 10^5$ - $2 \times 10^6$ A/cm$^2$ sr at a cathode temperature of 1800K [29,78]. In addition, the brightness of the thermionic cathodes is achieved at relatively high voltages, about 20kV, whereas the field emission cathode can achieve its high brightness at much lower voltages, with typical operating voltages lying in the range of 3-6kV. The field emitter has a very small radius of curvature, typically 0.01-0.3 μm. The current distribution from a field emission cathode is usually contained with a cone of half angle of 20 degrees [71].

The disadvantages of the field emission electron sources are in their large current fluctuations, which are strongly affected by the operating conditions [18,69,80,88].

In a thermionic emission cathode, electrons do not meet an accelerating field at the cathode surface, thus their velocity is very low and they create a space charge just in front of the cathode surface. The electric field due to this space

charge decelerates emitted electrons, so that the surface potential barrier, i.e. the work function barrier, is effectively increased. Therefore, the emission current is prevented from increasing. This effect can be considered as a kind of negative feedback, which increases the stability of a system, as is familiar in feedback amplifiers and in servo-systems. Thus the thermionic cathode has a stabilizing mechanism by nature under typical operating conditions.

In the case of a field emission cathode, electrons always meet an accelerating field and cannot be expected to create such a high level of space charge. The low level of the space charge, i.e. low level of stabilization, makes the emission current very noisy and with very high fluctuations as a consequence. The surface conditions of the cathode directly influence the emission current. It is therefore necessary to study the noise generation mechanisms in order to approach a stable field emission electron source.

## Current Fluctuations in a Field Emitter

Field emission occurs when a strong accelerating electric field is applied to a cathode. To make such a strong electric field, typically $5 \times 10^7$ V/cm, a field emitter is made in the form of a sharp needle, whose apex radius is less than 1 μm as shown in Figure 1. Taking into account the field and the electron image forces, the potential barrier is both lowered and narrowed as shown in Figure 2. Then it is possible for electrons to tunnel out through the barrier. The emission current density J (A/cm$^2$) obeys the Fowler-Nordheim equation [36,88]

$$J = 1.54 \times 10^{-6} \frac{F^2}{\phi\, t^2} \exp\left(-6.83 \times 10^7 \frac{\phi^{3/2} v}{F}\right) \quad (1)$$

where F (V/cm) is the applied electric field and $\phi$ (eV) is the work function. The quantities t and v are slowly varying functions of F and $\phi$. For $\phi$ in the range of 2.0 to 7.0 eV, and for J in the range of 1.0 to $10^7$ A/cm$^2$, t varies from 1.03 to 1.08, while v varies from 0.3 to 0.8. Typically, for field emission from tungsten, v is in the range of 0.61 to 0.69 [88]. By setting t = 1.05 and v = 0.65 a simpler expression can be obtained [36],

$$J = 1.4 \times 10^{-6} \left(\frac{F^2}{\phi}\right) \exp\left(-4.44 \times 10^7 \frac{\phi^{3/2}}{F}\right) \quad (2)$$

Introducing a geometrical factor β, which relates F to applied voltage V through

$$F = \beta V \quad (3)$$

equation (2) becomes [49]

$$J = \frac{B \beta^2 V^2}{\phi} \exp\left(-\frac{C \phi^{3/2}}{\beta V}\right) \quad (4)$$

where B and C are constants. Typically β is approximated by [75]

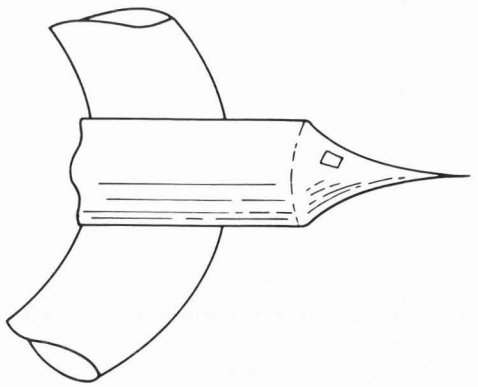

Figure 1. A typical tungsten field emission cathode structure. The electropolished tip is welded to a tungsten hairpin filament.

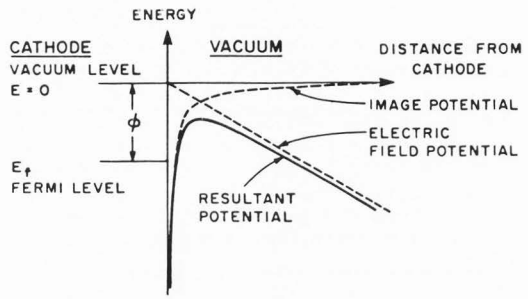


Figure 2. Potential energy diagram for the cathode-vacuum interface with an accelerating electric field. The image potential is the barrier for the zero field case.

$$\beta = \frac{1}{5\, r} \quad (5)$$

where r is the emitter apex radius.

For a typical field strength of $5 \times 10^7$ V/cm and a work function of 4.5 eV, a 1% change in β, i.e. in r, results in about a 15% change in J, with $\phi$ and V remaining constant. For the same field and work function, a 1% change in $\phi$ results in a change of about 20% in J, with β and V remaining constant [49,62]. Clearly, both β and $\phi$ must be carefully controlled in order to stabilize the emission current.

A typical current variation of a tungsten field emitter with time, with V remaining constant, is shown in Figure 3(a) [36,69]. Before the accelerating voltage is applied, the emitter is "flashed" or heated with a short current pulse through the filament, which supports the emitter tip. Just after flashing, the surface of the field emitter is clean and smooth, so that the emission current is very large. The current decays due to gas adsorption, which increases the work function. After the initial decay, the current stabilizes typically at about 10% of the initial value and remains almost constant for

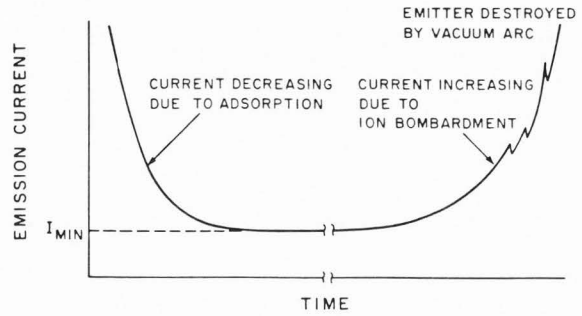


Figure 3(a). A typical current variation of a tungsten field emitter with time, with V remaining constant. (After Swann and Smith [69]).

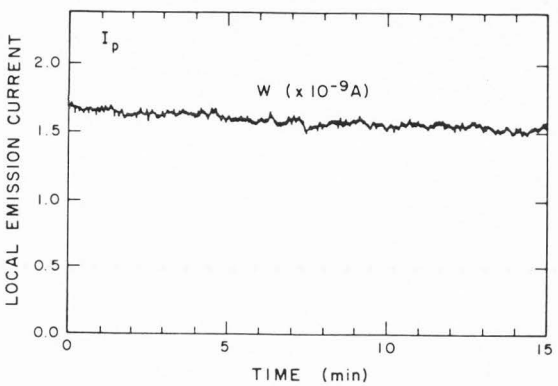


Figure 3(b). Typical random fluctuations in the stable period after the initial decay. The electrons were collected by a probe hole with a cone half angle 1.9 degrees. (After Adachi et al [2]).

several hours, although this largely depends on the operating conditions. Even in this stable period, emission current fluctuations of 2-5% are typical for a moderately high vacuum of $10^{-9}$ Torr ($1.33 \times 10^{-7}$ Pa) [36]. After the stable period, drastic increases in fluctuations are observed in the current, which are caused by the sputtering at the cathode apex due to ion bombardment of the residual gas, and finally these are followed by a destructive vacuum arc [18,36,69,88].

As mentioned previously, adsorbed molecules can change the work function appreciably. The change due to adsorbed nitrogen is an increase of 0.5 eV [36]. This causes about a 15 fold decrease in the emission current. Assuming that the electron emission from a surface with adsorbed gas molecules is so small that the emission current is roughly proportional to the clean portion of the surface, that is,

$$\frac{I}{I_0} = 1 - \theta \tag{6}$$

the initial decay of the current is given by [80]

$$\frac{I(t)}{I_0} = (1 - \theta_e) + \theta_e \exp\left(-\frac{t}{t_0}\right) \tag{7}$$

with the damping time

$$t_0 = \frac{n_0}{N_I \beta_I} \tag{8}$$

and the ultimate coverage

$$\theta_e = \frac{n_G S(\theta)}{N_I \beta_I} \tag{9}$$

where $\theta = n/n_0$ is the surface coverage, $n_0(cm^{-2})$ is the maximum surface density of the adsorbed gas molecules, $N_I$ ($cm^{-2}$ $sec^{-1}$) is the number of bombarding ions per unit time at the emitter surface, $\beta_I$ is the rate at which the adsorbed molecules are desorbed by the ion bombardment, $n_G$ ($cm^{-2}$ $sec^{-1}$) is the number of bombarding gas molecules per unit time and $S(\theta)$ is the sticking probability of the gas molecules. The calculated results are in good agreement with experimentally measured results [80].

Short term fluctuations are included in both the initial decay and the following period of constant current. Typical current fluctuation from a tungsten field emitter is shown in Figure 3(b) [2]. Two factors contribute to this current fluctuation. Ion bombardment of the residual gas molecules and migration of the adsorbed gas molecules. Thus the relative fluctuation can be expressed by

$$\frac{\Delta I}{I} = f(N_I) + c \tag{10}$$

where the first term is due to the ion bombardment and the second the migration [80].

The bombarding ions are formed by stimulated desorption of gas molecules at the anode surface [69,75] and also by electron collisions with the residual gas molecules in the space between the cathode and the anode. Calculations of the ion trajectories show that approximately $10^{-10}$ to $10^{-9}$ of the ions formed at the anode surface can reach the emitter tip and that only the ions generated in the space within a few micrometers around the apex are able to impinge on the emitting area [63,66]. Considering the two factors, $N_I$ can be expressed by [80]

$$N_I = 3.1 \times 10^{18} \beta_e \left(\frac{n_a r_0}{R}\right)^2 I + 1.7 \times 10^{33} \sigma_G (r_1 - r_0) I P \tag{11}$$

where $\beta_e$ ($cm^{-2}$ $sec^{-1}$) is the rate at which ions are ejected by electron bombardment, $n_a r_0$ is an apparent ion source radius ($n_a = 10$), $r_0$ is the cathode apex radius, R is the distance between the cathode and the anode, $\sigma_G$ ($cm^2$) is the electron impact ionization cross section, $r_1$ (1.4 μm) is the effective radius in which all

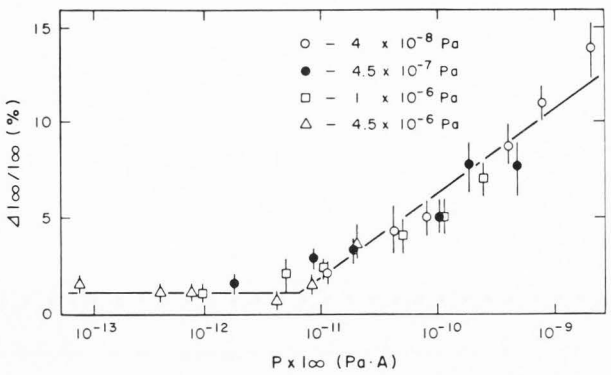


Figure 4. Relative fluctuations of a field emission current from W, plotted as a function of the product $I_t P$. (After Todokoro et al [80]).

ionized molecules can strike the emitting area [63,66], and P(Pa) is the residual gas pressure.

Thus the first term, the contribution of the ions created at the anode, is proportional to the emission current I, and the second term, the contribution of the ionized residual gas molecules, is proportional to the product IP. In a typical case with R = 1 cm, $\beta_e = 10^{-5}$ and $\sigma_c = 10^{-16}$ cm$^2$, the second term is predominant if the residual gas is higher than $1.8 \times 10^{-8}$ Pa, that is, the ion bombardment due to the residual gas molecules is predominant, so that the relative fluctuation is a function of the product IP. A typical experimental result shown in Figure 4 indicates that the relative fluctuation is proportional to the logarithm of the product IP above $7 \times 10^{-12}$ (PaA). Below this point the relative fluctuation is almost constant and is attributed to the migration of the adsorbed gas molecules at the emitter surface [80].

The critical pressure of $1.8 \times 10^{-8}$ Pa [80] is reduced if $\beta_e$ has a smaller value or the adsorbed gas at the anode surface has been completely

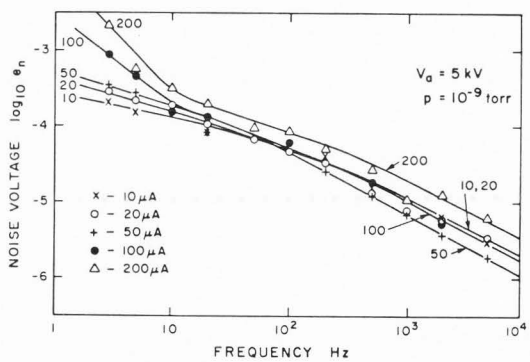


Figure 5. Spectral content W field emission current noise in terms of noise spectral density $e_n$ (V/Hz$^{0.5}$). (After Swann and Smith [69]).

removed. $N_I$ contributes also to the damping time $t_0$ through equation (8). When the second term of equation (11) is predominant, the product of $Pt_0$ is independent of the residual gas pressure, with I remaining constant. According to the experimental results of Oshima et al, the product $Pt_0$ of a W field emitter is constant up to an ultra high vacuum of $10^{-10}$ Pa, where the emission current is very stable, but a current fluctuation of less than 0.3% still remains. This current fluctuation is attributed to the surface migration of impurity atoms such as carbon and/or tungsten atoms [60]. In such a high vacuum an emitter life of greater than 12000 hours has been demonstrated [23,49].

The current fluctuation due to ion bombardment is a function of the emission current, while the current fluctuation due to migration of the adsorbed gas molecules is independent of the emission current. The noise increases monotonically with emission current only for very low frequencies as shown in Figure 5 [69]. Thus the noise for higher frequencies is due to migration of the adsorbed gas molecules. 1/f dependence of the noise is a characteristic feature of flicker noise, which is due to statistical motion of the adsorbed molecules on the emitter surface. The noise has been analyzed by studying equilibrium adsorbate density fluctuations in a small "probed" region of a field emitter [34,35].

The threshold temperature for current fluctuation of W is 300, 650, 1000K for the (310), (112) and (100) planes respectively, showing a significant decrease with decreasing atomic density of the respective crystal planes [72], whereas the work function shows a significant decrease with decreasing atomic density. Thus the emission current from a low work function plane of W includes a high level of fluctuations [36].

The emission current and noise in the steady period increase slightly with time. This is followed by drastic increases of current and noise, which finally becomes a destructive vacuum arc [18,36,49,69]. These current fluctuations are due to surface damage caused by ion bombardment leading to enhanced local fields [49]. In such regions there is an increased probability of electron emission, and possibly of ion bombardment also, and these effects tend to increase the noise.

In the ordinary case, flashing is performed to smooth the damaged surface and to desorb the adsorbed gas molecules before the drastic increase of current occurs [49]. Thus a periodic flashing is essential for stable operation [36].

Most of the current fluctuations are caused by interaction of the emitter surface with the residual gas as mentioned above, so that it is essential to reduce this interaction in order to reduce the current fluctuations [23,62].

The direct approach to a stable field emission source may be to utilize an extreme ultra-high vacuum system which is very expensive and is very delicate to use. There is also the difficulty of equipping such a vacuum system with an electron optical system. The stringency of the vacuum has prevented the field emission electron source from being widely applied.

Recently, a vacuum system made of aluminum alloy has been developed and now is commercially available [39,40]. In comparison with a conventional stainless steel system, this system has advantages of (1) a lower temperature and a shorter time are required for the baking, (2) a lower rate of gas adsorption, (3) light weight, (4) a lower load to vacuum pumps, (5) a low ultimate residual gas pressure of less than $10^{-9}$ Pa and (6) being perfectly nonmagnetic. Thus the aluminum alloy vacuum system may have the potential to solve the vacuum problem, but still may be very delicate to use.

From a practical view point, stabilization of field emission current with an electronic feedback circuit can be performed. Field emission current is a strong function of the accelerating voltage according to equation (4). However, the emission current cannot be controlled by changing the anode voltage, because the energy of the emitted electrons changes depending on the anode voltage. An additional electrode is necessary for such a purpose as shown in Figure 6. The electrode is called a source control aperture [56], or Wehnelt [51], or an emission control electrode [16,17]. The applied voltage of the electrode is slightly lower than the equipotential line at the position. The electric field just in front of the emitter can be controlled by changing the voltage of the control electrode, so that total emission current can be controlled without changing the electron energy. By detecting the total emission current, the feedback signal to the control electrode can be made and the emission current successfully stabilized as shown in Figure 7 [51].

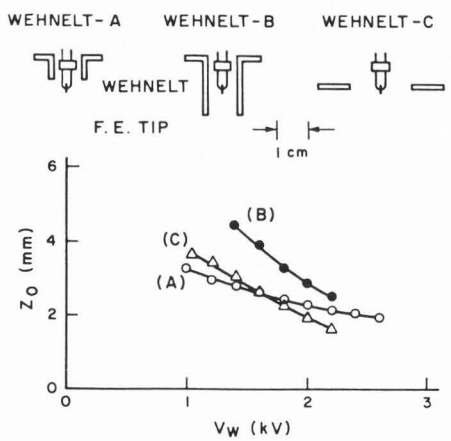


Figure 6. Axial shift $z_0$ of the virtual electron source caused by the change in the control electrode (Wehnelt) voltage for three different electrode configurations. (After Nomura et al [51]).

The axial position of the virtual source shifts due to the change of the electron trajectories, because the electric field distribution between the emitter and the anode is changed by the potential of the control electrode. The amount of the shift depends largely on the

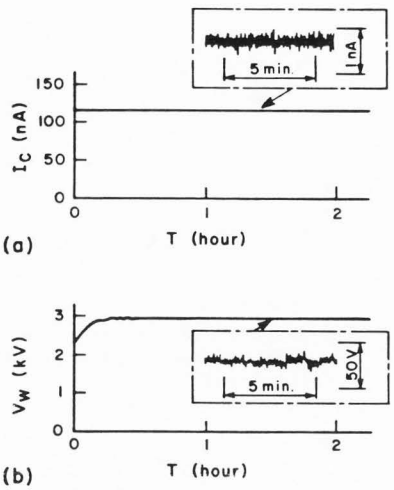


Figure 7(a) Stabilized current by an electronic feedback circuit and
7(b) the voltage appearing on the control electrode. (After Nomura et al [51]).

electrode configuration as shown in Figure 6. If a hemi-spherical anode is adopted, the defocusing due to the shift can be almost comparable to the level of defocusing due to the chromatic aberration and/or the diffraction of the field emission gun [51]. Recently, methods for numerical analysis of point electron sources have improved [41,42], and new electrostatic lenses proposed [54,55], so that the optimum configuration for the minimum shifts can be expected.

The fluctuations of the total emission current do not necessarily correspond to the fluctuations of the probe current or the beam current. There is no strict correlation between them. Thus it is necessary to detect the fluctuation of the beam current to effect a complete stabilization; but it is impossible to detect the fluctuation of the beam current directly, because the beam itself is used for the purpose of the electron beam system. Cleaver [17] detected the current fluctuation of the near axial component of the electron beam by a beam monitor electrode placed just beneath the anode and got a sufficient stability for the production of satisfactory micrographs from specimens of normal contrast. However, the stabilization has some optical consequences which degrade the system performance.

## New Materials for Field Emission Sources

The materials for field emitters should be of high melting point, of low vapor pressure at high temperature, of low electrical resistivity, of low work function, chemically stable, highly resistive to ion bombardment and mechanically hard. It is necessary to be able to make a fine, sharp needle easily. The high melting point and low value of work function are the same

requirements as for a thermionic cathode. Many materials are evaluated by defining a figure of merit, which is based on the Richardson-Dushman equation [96]. The figure of merit is

$$F = 2 \log T_m - 5 \times 10^3 \frac{\phi}{T_m} \qquad (12)$$

where $T_m$ (K) is the melting point, $\phi$ (eV) is the work function. Although this figure of merit directly gives a measure of thermionic emission current, it also gives a measure of thermal field emission current [96]. The larger the value, the more suitable the material is for a high brightness cathode. A negative value means that the material is not suitable for a cathode. Although the highest working temperature of a cathode does not equal the melting point, comparison between many kinds of materials is possible as a consequence of adopting the melting point as a measure of the highest working temperature. The materials with high values of the figure of merit are listed in Table 1, where $T_p$ (K) is a temperature at which the material has a vapor pressure of $10^{-5}$ Torr ($1.33 \times 10^{-3}$ Pa), and A is the Richardson constant.

Oxides have a very high electrical resistivity, so that they are not suitable for field emission sources.

Tungsten, which is widely utilized for field emission cathodes, has a rather high work function. According to equation (1), the higher the work function, the stronger the required applied electric field must be. As a consequence, a strong electrostatic force is present at the apex of the field emitter. Thus high mechanical strength is required for a field emitter. Hardness can be a measure of the mechanical strength. W has a rather small value of hardness, whereas $LaB_6$, and carbides have large values. So far no successful efforts have been reported for stable field electron emission from $LaB_6$, although it shows superior characteristics as a thermionic cathode. According to this author's experience, the noise level was higher than that for W. The reason why the $LaB_6$ field emitter is unstable does not seem to be known.

Carbon is excluded from the evaluation because it has many crystallographic phases and the work function changes very much from phase to phase. However, carbon has a very high melting point, and so there have been many attempts to apply it as a field emission cathode [5,6,30,38,47,48,91]. The current fluctuation is step and spike-like and a low level of random noise is included. The sticking probability of gas adsorption on carbon is very low [9] and the low level of the random noise can be attributed to the low level of gas adsorption. It gives stable electron emission, especially in the thermal field emission mode. The emission mechanism is not a simple "metallic" process, but it includes some "semiconductor like" processes [47].

Carbides of transition metals have rather small values for the work function. The melting points are extremely high, which make the figures of merit very high. Much work has been done on field emission from TiC [2,3,20,31,43,61,79]. The stable field emission from a TiC single crystal is shown in Figure 8. No current fluctuations are observed after the slight initial decay [28]. The total emission current $I_t$ was about 4.5 μA, which can be large enough for an ordinary electron beam probe system. $I_p$ is the probe current, collected by a probe hole with a cone half angle of 1.9 degrees. Current fluctuations are observed if the flashing condition is not adequate or the emission current level is high as shown in Figure 9, where the total emission current was 18 μA, which is four times as large as that of Figure 8 [28].

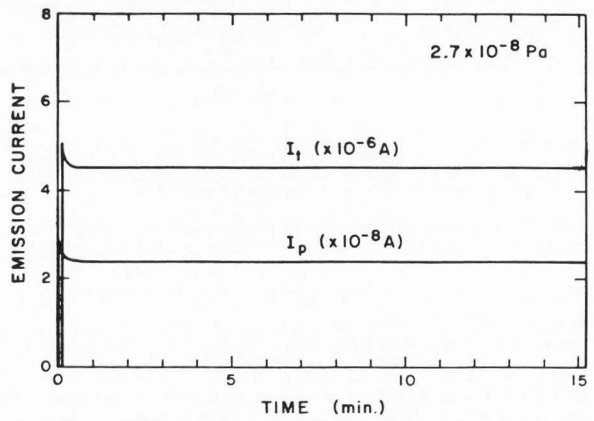


Figure 8. Stable field emission current from a TiC single crystal processed by the optimum flashing. $I_t$ is the total current and $I_p$ is the probe current collected by a probe hole with a cone half angle of 1.9 degrees. (After Fujii et al [28]).

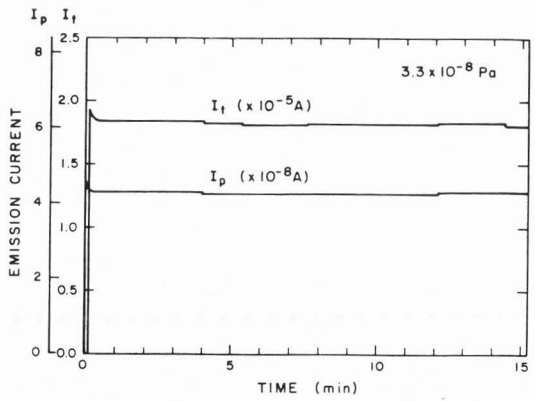


Figure 9. Step like current fluctuations in field emission current from a TiC single crystal with a high total emission current of 18 μA. (After Fujii et al [28]).

It is worth noting that the current fluctuations from carbides are fundamentally step-like and do not include flicker (1/f) noise. This is in contrast with the W field emitter, whose field emission current always includes flicker noise. The stability of the emission current is largely dependent on the flashing conditions and there is an optimum flashing temperature [2,3,28,61].

The emission patterns change with the flashing temperature. There are five distinct temperature regions which give different emission patterns. Stable field emission was obtained when the flashing temperature was in a region between 1900 and 2100 C. Although a symmetrical pattern is also observed in a region between 1500 and 1700 C, the emission current was not stable. A flashing temperature higher than 2100 C gives rather high levels of current fluctuations [2,3, 28].

The optimum flashing temperature depends on the method used in the flashing process. The optimum flashing temperature reported by Oshima et al was in a region of 1700 to 1900 C [61]. The flashing process of Oshima et al was the following: flashing for several seconds was repeated with an interval of a few minutes for a full day or longer. The flashing process of Fujii et al [2,3,28] is the following: after a pressure of less than $10^{-8}$ Pa was reached, the field emitter was heated for 5 - 15 sec. Then the emitter was cooled to room temperature. Successive flashing was performed after the vacuum had recovered to a pressure less than $10^{-8}$ Pa. The flashing process was repeated until the base pressure did not increase to more than $10^{-8}$ Pa.

The physical process for the optimum flashing temperature has not been understood. The reason why Oshima et al adopted their flashing process is that the field emitter was supported by carbon block heaters, as in the Vogel type support for the $LaB_6$ cathode [86]. The carbon block heater is very porous, and contains a large amount of gas which escapes very slowly, so that a long flashing time is required. Whereas the tip of Fujii et al was supported by a Ta ribbon, which contains much less adsorbed gas than the carbon blocks.

The current fluctuations are always followed by flickering of the emission patterns. The current steps of the total current of Figure 9 do not correspond to the current steps of the probe current. The step in the probe current occurs when the bright spot over the probe hole flickered.

The number of the current fluctuations appearing over a period of 20 minutes is clearly a function of the product $I_tP$ as shown in Figure 10. As mentioned above, when the residual gas pressure is higher than the critical pressure of $1.8 \times 10^{-8}$ Pa, the second term of equation (11) is dominant, so that the number of ions which bombard the emitter surface is a function of the product IP. Thus the current fluctuations are caused by ion bombardment due to the residual gas molecules. The figure also shows that the optimum flashing process reduces the frequency of the current fluctuations by 1/40 (98%) [2,28].

The bright spots of the emission patterns correspond to the (110) direction of the crystal [2,3,28]. Futamoto et al [31] suggested that the bright spots correspond to (110) facets. Examining the emission patterns of both (100) and (111) oriented field emitters, Fujii et al concluded that the electron emission occurs at the sharp edges between (111) and (001) facets and no stable (110) facets are expected [28]. Field emission of electrons will occur only at sharp edges of facets and not on the facets, if the temperature is low [73].

The lack of flicker noise (1/f noise) is due to the low probability of gas adsorption on the carbides and the formation of no mobile physisorbed precursor to chemisorption [32,33,59 95]. It also is due to the small changes in work function arising from gas adsorption [58,59,96]. The oxygen peak height of XPS (X-ray photoelectron spectroscopy) increases with increasing exposure of $O_2$, and saturates above 3000L (L: Langmuir = $10^{-6}$ Torr sec); correspondingly, the work function increases monotonically from 3.8 to 4.2 eV [58]. These changes in both the sticking probability and the work function are much smaller than those of W (001), where the saturation of oxygen chemisorption occurs at 30L which results in a change of the work function from 4.6 to 6.2 eV [59].

The quality of the crystal is also important for stable field emission current. A crystal which gave stable field emission was grown by a floating zone melting method under a high pressure helium atmosphere [28]. Multiple passes of the zone were performed to reduce the impurity level. The stoichiometry of the crystal is also important. Stoichiometric TiC shows a small change in work function due to oxygen adsorption [95]. The crystals with chemical composition of 0.95 and 0.96 gave the most stable field emission current [28].

Low probability of gas adsorption is also reported on TaC [32,33]. It seems that low probability of gas adsorption is a common feature of transition metal carbides. Current fluctuations in field emission from TaC are also step like and contain no flicker (1/f) noise [93]. These features are the same as TiC. Essentially the same features can be expected for the other carbides shown in Table 1.

TiC has the lowest melting point among the carbides listed in Table 1. This means that TiC is the easiest carbide from which to grow a high quality single crystal. TaC and HfC have the highest melting points, so that they are very difficult to grow a high quality single crystal from, although a high melting point is a desirable characteristic for a field emitter.

Carburization of a pure metal provides an easy way to make a field emitter. TaC made by carburization of a Ta metal needle was sometimes single crystalline, although the emission current contained large fluctuations [93]. Reduction of the fluctuations can be expected by improving the technique.

The hardness of TiC is reduced drastically by heating it to about 1000 C, but that of TaC is not [4], although the hardness of TaC is rather low at room temperature. While the flashing process of a W field emitter anneals the damaged surface, it is not certain at present that this

Table 1. Properties of Electron Sources.

| Material | F | $\phi$ (eV) | $T_m$ (C) | $T_p$ (C) | A ($A/cm^2K^2$) | Resistivity ($\Omega$ cm,20C) | Hardness ($kg/mm^2$) |
|---|---|---|---|---|---|---|---|
| LaB | 1.49 | 2.69 | 2530 | 1610 | 29-120 | $1.5 \times 10^{-5}$ | 2470 |
| (110) | 1.67 | 2.60 | 2530 | 1610 | 82 | $1.5 \times 10^{-5}$ | 2470 |
| $CeB_6$ | 0.76 | 2.73 | 2290 | .... | 3.6, 580 | $2.9 \times 10^{-5}$ | (3140) |
| (110) | 0.98 | 2.63 | 2290 | .... | ..... | $2.9 \times 10^{-5}$ | (3140) |
| $YB_4$ | 2.23 | 2.61 | 2800 | .... | 0.1, 0.045 | $2.9 \times 10^{-5}$ | ..... |
| $GdB_4$ | 3.11 | 1.98 | 2650 | .... | $10^{-4}$ | $3.1 \times 10^{-5}$ | ..... |
| TiC | 1.75 | 3.32 | 3160 | 2000 | 2.5 | $5.3 \times 10^{-5}$ | 2930 |
| ZrC | 2.31 | 3.38 | 3530 | 2240 | 0.2-140 | $6.2 \times 10^{-5}$ | 2860 |
| NbC | 2.40 | 3.45 | 3650 | 2250 | $10^{-6}$ | $5.1 \times 10^{-5}$ | 2400 |
| HfC | 2.81 | 3.40 | 3890 | 2300 | 0.3-40 | $4.5 \times 10^{-5}$ | 2860 |
| TaC | 2.53 | 3.61 | 3880 | 2380 | 0.22-2.1 | $4.1 \times 10^{-5}$ | 1570 |
| $CeC_2$ | 1.91 | 2.49 | 2540 | 1880 | ..... | $6.0 \times 10^{-5}$ | ..... |
| CaO | 3.36 | 1.78 | 2570 | 1542 | $10^{-2}$ | 2.8 (800C) | 560 |
| SrO | 3.83 | 1.43 | 2430 | 1430 | $10^{-3}$ | 18.0 (800C) | ..... |
| BaO | 3.31 | 1.25 | 1920 | 1128 | $10^{-2}$-$10^{-1}$ | 4.6 (800C) | ..... |
| $ThO_2$ | 2.65 | 2.78 | 3190 | 2200 | 2.5-160 | 0.65 (800C) | 945 |
| W | 0.41 | 4.54 | 3410 | 2560 | 60-100 | $5.5 \times 10^{-5}$ | 300 |

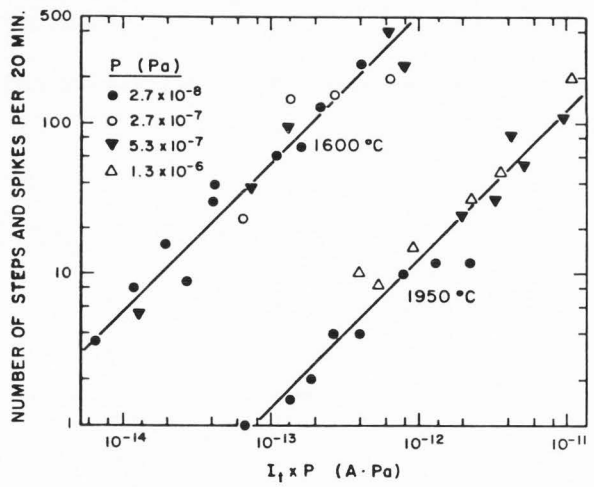


Figure 10. Number of step and spike-like fluctuations in the field emission current from TiC appearing for a period of 20 minutes for two different flashing temperatures of 1600 and 1950 C plotted against the product $I_tP$. (After Adachi et al [2]).

characteristic of TiC plays an essential role in the flashing process to reduce the current fluctuations.

The characteristic feature of TaC that the hardness does not decrease at high temperatures may suggest a potential usefulness of TaC for a thermal field emitter, as will be discussed later.

## Thermal field emission

Another way to reduce the interaction with the residual gas is to increase the emitter temperature. The advantages of thermal field emission consist primarily of relaxation of vacuum requirements, and higher operational current density and beam brightness [76]. The disadvantages are the large amplitude of low frequency noise [76,84] and a greater spread of kinetic energy of the electron beam [23,25,76,92,94]. When the temperature is high, $\theta_e$ of equation (9) has a small value, because the sticking probability $S(\theta)$ for the gas molecules is reduced. In fact fluctuations in the emission current from a glassy carbon field emitter have been reported to be reduced dramatically [91].

In the case of a tungsten field emitter, heating causes the "build up" which results in a destructive vacuum arc. Heating a field emitter in the absence of an applied field causes the emitter radius to increase due to the surface tension and the surface migration of the atoms ("dulling") [12]. In the presence of an applied field, the electrostatic force acts in opposition to the dulling force, so that the dulling rate will decrease. Then the dulling rate is given by

$$\left(\frac{dr}{dt}\right)_F = \left(1 - \frac{r F^2}{8 \pi \gamma}\right) \left(\frac{dr}{dt}\right)_0 \qquad (13)$$

where $\gamma$ is the surface tension and $(dr/dt)_0$ is the dulling rate without the applied field [7,11, 49].

For clean tungsten, the condition for $(dr/dt)_F = 0$ is given by

$$F_0 = 8.1 \times 10^4 / r^{1/2} \quad (V/cm) \qquad (14)$$

where r is in cm. Lower field strength than $F_0$ is necessary to avoid "build up". For an ordinary field emission tip with radius of 100 nm to 1 μm, $F_0$ corresponds to the range $8.1 \times 10^6$ to $2.6 \times 10^7$ V/cm. The useful range of the current densities ($10^4$ to $10^8$ A/cm$^2$) corresponds to fields in the range $4 \times 10^7$ to $8 \times 10^7$ V/cm, which is higher than the critical field $F_0$. Thus, the possibility of stabilizing the smooth emitter shape during thermal field operation of a smooth and clean tungsten emitter is eliminated [75].

Reduction of the work function is necessary to reduce the required applied field, according to equation (1). The work function of W (100) surface with an overlayer of Zr has a very small value of 2.6 eV in the presence of oxygen [65]. An applied field of $F = 2 \times 10^7$ V/cm gives a useful current density of about $5.3 \times 10^5$ A/cm$^2$ and an apex radius of 0.164 μm. These are practical values [75].

The characteristics of the ZrO/W thermal field emission cathode have been systematically examined mainly by Swanson's group [73,75,76,90] and it has been successfully applied to some microbeam equipment [82]. Zr on the surface of W forms a Zr-O composite that does not evaporate even at a high temperature of 2000 K [22]. The low value of the work function of ZrO/W(100) is due to formation of Zr-O composites. Metallic Zr has a rather high value of the work function. Auger percent compositions of W, Zr, O and N do not change with heating temperature up to 1800 K, whereas the work function decreases with the heating temperature as shown in Figure 11 [22].

The optimum operating temperature of the ZrO/W thermal field emission cathode is about 1800 K [73,75,90]. The emission current includes flicker (1/f) noise with current fluctuations less than 0.23% in the frequency interval 1 to 5000 Hz [73]. Higher levels of current fluctuations than flicker (1/f) noise are found at very low frequencies and this component is temperature, field and emitter geometry dependent [83]. A typical spectrum of the noise is shown in Figure 12 [73,77]. Relatively high noise levels have been reported by other authors [24, 79], suggesting that special care is necessary for stable operation. The flicker noise in the thermal field emission current suggests that the migration of atoms at the cathode surface still plays an important role in the noise generating mechanism.

The energy spread of thermal field emission electrons has a larger value than either thermionic or cold field emission [1,10,25,92,94]. Thus the FWHM (full width of half maximum) has a maximum value at a certain temperature $T_c$, with the emission current remaining constant as shown in Figure 13 [1]. The origin of the maximum is

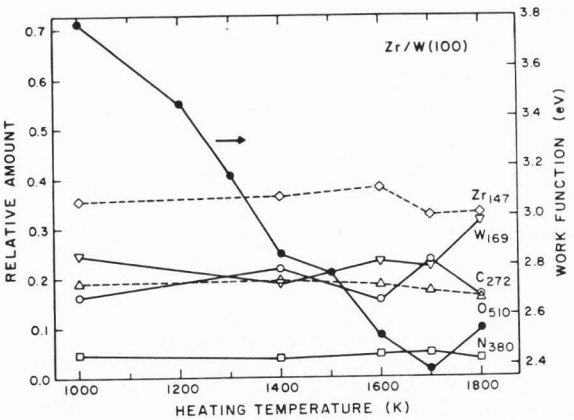


Figure 11. Auger percent compositions of W, Zr, C, O and N, and the work function $\phi$ versus temperature of a ZrO/W(100) cathode surface. Points at 1000K were obtained after a $10^{-5}$ Torr sec (= 10L) oxygen dose including several monolayers of zirconium. (After Danielson and Swanson [22]).

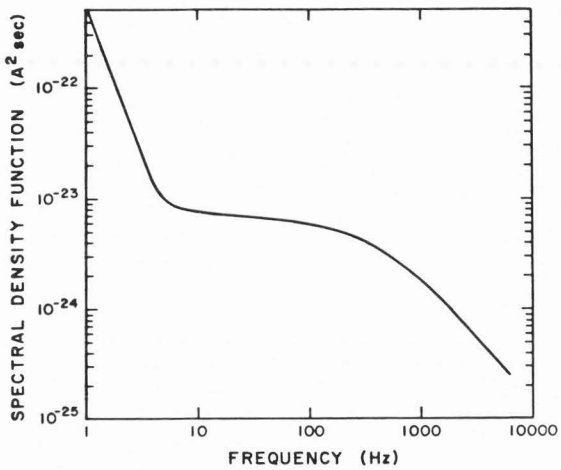


Figure 12. Spectral density function of the noise from a Zr/W(100) thermal field emitter (V = 7.5 kV; T = 1800K). The solid angle subtended at the emitter by the acceptance aperture was 0.113 msr and the transmitted (probed) current was 30 nA. (After Swanson et al [77]).

as follows [10]: at a low temperature, a high field is necessary and emission is dominated by emission from the vicinity of the Fermi level, whereas at a high temperature, a low field is necessary and emission is confined to the top of the work function barrier. On the other hand, at intermediate temperature, intermediate field is necessary and comparable emission occurs in the region of the Fermi level and the top of the work function barrier, leading to the maximum. Thus

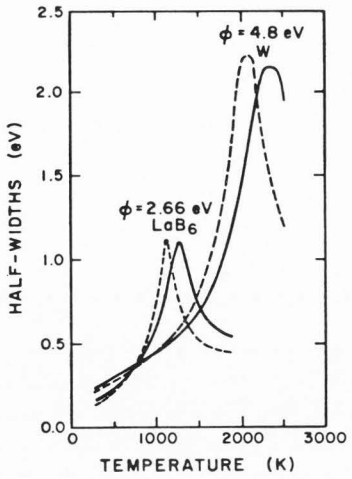


Figure 13. Calculated results of the half widths of total energy distribution of thermal field emitted electrons with two different work functions of 2.66 eV ($LaB_6$) and 4.8 eV (W) for two current densities of $10^5$ (solid curves) and $10^4$ (dashed curves) A/cm$^2$. (After Adachi et al [1]).

at a higher temperature than $T_c$, contribution of the emission at the top of the work function barrier is dominant.

In case of the ZrO/W thermal field emitter, the optimum operating temperature is about 1800 K, which is higher than $T_c$, so that electron emission occurs mainly at the top of the work function barrier and the FWHM of the energy spread of the emitted current has a small value [73]. Often it is operated in the extended Schottky emission mode rather than the thermal field emission mode [73,74]. In consequence, a smaller applied field is necessary and the radius of the apex can be large, say a few micrometers, which can still be small enough for fine focused electron beams. The small applied field and large radius of the apex give a low rate of the "build up" and then a long life time can be expected. A life time of 5000 hours was reported [73]. The large radius of the apex gives a low level of current density at the cathode surface, thus the broadening of the energy distribution due to Coulomb interaction of the electrons is reduced [10]. A low voltage field emission (i.e. Schottky emission) mode of ZrO/W gives equivalent spatial resolution to a room temperature field emission mode of W [83].

When a W (100) field emitter is flashed in the presence of a positive applied field of $5 - 6 \times 10^7$ V/cm [18,71], or the emitter is exposed for about 5 sec to oxygen at a pressure of $10^{-6}$ Torr ($1.33 \times 10^{-4}$ Pa) and heated in a vacuum less than $10^{-9}$ Torr ($1.33 \times 10^{-7}$ Pa) at a temperature of 1200 - 1400 C [84], "build up" occurs. The apex radius of the built-up cathode is so small that a low accelerating voltage is necessary. The emitted electrons are confined to a narrow beam with a half angle of less than 9 degrees, therefore a reduction of the emitted current is required for fine focusing of a normal field electron source [71]. The atomic density of W(100) is high so that the emission current fluctuations are rather low levels. Comparing the noise levels between the ZrO/W Schottky emitter and the W (100) built-up thermal field emitter at similar values of the geometric factor and angular intensity, ZrO/W exhibits an almost 10 times reduction in $\Delta I/I$. This is attributed to the inherently small emitting area of the built-up emitter, when viewed through a specified beam aperture angle [76].

The current fluctuations of a glassy carbon thermal field emitter are step and spike-like and no flicker noise is included [38]. The frequency of the current fluctuation is a function of the product IP. As stated above this is the characteristic feature of the current fluctuation originating from desorption and adsorption of the residual gas molecules stimulated by the ion bombardment at the emitter surface [80]. The disadvantage is in the low strength of crystal structure. Carbon has many stable structures, and none of these structures is compact atomically. The compact crystal of carbon is diamond, which is an insulator.

The same type of current fluctuation is observed in the cold field emission current from carbides of transition metals such as TaC, TiC and ZrC. TaC has a high value of hardness even at a high temperature of 1000 C [4], which is an advantage for operation in the thermal field emission mode. The work functions of TiC and ZrC are reported to be reduced slightly with heating after exposing to oxygen [27]. Thus transition metal carbides can be expected to show good characteristics in thermal field emission.

## Summary

The current fluctuations of a field emission electron source are mainly due to the interaction of the emitter surface with the residual gas molecules. Thus a direct way to reduce the current fluctuations may be to utilize an extremely high vacuum system, which is very expensive and delicate to use; it does not seem to be practical. Stabilization of the emission current by an electronic feedback circuit can be performed, but it requires the incorporation of an additional electrode, i.e. a control electrode. Changes in the potential of the control electrode induce some optical consequences which degrade the system performance.

New materials for field emission cathodes are evaluated and carbides of transition metals are shown to have potential values for use as stable field emitters. Stable field emission has been reported on TiC single crystals. So far only a few fundamental experiments have been reported on the stable field emission from the carbides. The carbides are also expected to have superior characteristics as thermal field emitters.

Operation in the thermal field emission mode is another way to reduce the current fluctuation. The ZrO/W(100) thermal field emitter gives a stable field emission, whose fluctuation is less

than 0.23% in a frequency range of 1 to 5000 Hz. The only disadvantage is its relatively high fluctuation at very low frequency, which is believed to be caused by thermal instabilities.

Avoidance of a cathode heating power supply is sometimes desirable in a practical application of the high brightness electron sources. From this viewpoint, the thermal field emission mode has a disadvantage, and the cold field emission cathode is desirable. Although carbide field emitters have superior characteristics, they require further confirmation of their potential features from the view point of practical applications.

## Acknowledgements

The author wishes to thank Profs. L.W. Swanson and J. Orloff of the Oregon Graduate Center for the opportunity to prepare the manuscript, and for assistance in editing. Kind assistance of Dr. D. Tuggle is also greatly appreciated. The author thanks his colleagues of the Applied Materials Science Department of the Muroran Institute of Technology for their support during the absence of the author. The financial support provided by the Ministry of Education Japan is gratefully acknowledged.

## References

1 Adachi H, Shibuya Y, Hariu T, and Shibata Y. (1977). "Spread of Total Energy Distribution of Thermal Field Emitted Electrons from $LaB_6$," J. Phys. D: Appl. Phys. 10, L113-L115.

2. Adachi H, Fujii K, Zaima S, Shibata Y, Oshima C, Otani S, and Ishizawa Y. (1983). "Stable Carbide Field Emitter," Appl. Phys. Lett. 43, 702-703.

3. Adachi H, Fujii K, Zaima S, Shibata Y, and Otani S. (1984). "Flashing Temperature Dependence of Field Electron Emission from TiC Single Crystals," Shinku. 8, 658-666 (in Japanese).

4. Alison C, Hoffman M, and Williams WS. (1982). "Electron Energy Loss Spectroscopy of Carbon in Dissociated Dislocations in Tantalum Carbide," J. Appl. Phys. 53, 6757-6761.

5. Baker FS, Osborn AR, and Williams J. (1972). "Field Emission from Carbon Fibres, A New Electron Source," Nature, 239, 96-97.

6. Baker FS, Osborn AR, and Williams J. (1974). "The Carbon Fibre Field Emitter," J. Phys. D: Appl. Phys. 7, 2105-2115.

7. Barbour JP, Charbonnier FM, Dolan WW, Dyke WP, Martin EE and Trolan JK. (1960). "Determination of the Surface Tension and Surface Migration Constants for Tungsten," Phys. Rev. 117, 1452-1459.

8. Bauer B, and Speidel R. (1981). "Influence of Energy Spread of Field-Emitted Electrons on Resolution in the Scanning Transmission Microscope (STEM)," Ultramicroscopy 6, 281-286.

9. Beitel GA. (1972). "Adsorption of Carbon Monoxide and Hydrogen on Graphite," J. Vac. Sci. Technol., 9, 370-372.

10. Bell AE, and Swanson LW. (1979). "Total Energy Distribution of Field-Emitted Electrons at High Current Density," Phys. Rev. B19, 3353-3364.

11. Bettler PC, and Charbonnier FM. (1960). "Activation Energy for the Surface Migration of Tungsten in the Presence of a High Electric Field," Phys. Rev. 119, 85-93.

12. Boling JL, and Dolan WW. (1958). "Blunting of Tungsten Needles by Surface Diffusion," J. Appl. Phys. 29, 556-559.

13. Broers AN. (1973). "A New High-Resolution Electron Probe," J. Vac. Sci. Technol. 10, 979-982.

14. Broers AN. (1975). "Electron Sources for Scanning Electron Microscopy," Scanning Electron Microsc. 1975: 661-670.

15. Carpenter RW, and Bentley J. (1979). "On the Performance of a Field Emission Gun TEM/STEM," Scanning Electron Microsc. 1979; I: 153-160.

16. Cleaver JRA. (1975). "Field Emission Guns for Electron Probe Instruments," Int. J. Electronics 38, 513-529.

17. Cleaver JRA. (1975). "Stabilization of the Electron Probe Current in the Scanning Electron Microscope with a Field Emission Cathode," Int. J. Electronics 38, 531-540.

18. Crewe AV, Eggenberger DN, Wall J, and Welter LM. (1968). "Electron Gun Using a Field Emission Source," Rev. Sci. Inst. 39, 576-583.

19. Crewe AV, Wall J, and Welter LM. (1968). "A High-Resolution Scanning Transmission Electron Microscope," J. Appl. Phys., 39, 5861-5868.

20. Crewe AV, Isaacson M, and Johnson D. (1969). "A Simple Scanning Electron Microscope," Rev. Sci. Instrum., 40, 241-246.

21. Crewe AV. (1975). "Electron Microscopes Using Field Emission Source," Surface Science, 48, 152-160.

22. Danielson LR, and Swanson LW. (1979). "High Temperature Coadsorption Study of Zirconium and Oxygen on the W(100) Crystal Face," Surface Science, 88, 14-30.

23. Dyke WP, Charbonnier FM, Strayer RW, Floyd RL, Barbour JP, and Trolan JK. (1960). "Electrical Stability and Life of the Field Emission Cathode," J. Appl. Phys., 31, 790-805.

24. El-Gomati MM, Putton M, and Browning R. (1985). "An All-Electrostatic Small Beam Diameter, High Probe Current Field Emission Electron Probe," J. Phys. E: Sci. Instrum.,

18, 32-38.

25. El-Kareh AB, Wolfe JC, and Wolfe JE. (1977). "Contribution to the General Analysis of Field Emission," J. Appl. Phys., 48, 4749-4753.

26. Eriksson C, Wiklund B, and Astrand B. (1981). "A Thermal Heated Field Emitter Gun for E-Beam Exposure," Physica Scripta, 24, 477-481.

27. Fujii K, Zaima S, Adachi H, Otani S, Oshima C, Ishizawa Y, and Shibata Y. (1983). "Basic Field Emission Properties of TiC and ZrC Single Crystals," Shinku, 26, 251-258 (in Japanese).

28. Fujii K, Zaima S, Shibata Y, Adachi H, and Otani S. (1985). "Field Electron Emission Properties of TiC Single Crystals," J. Appl. Phys., 57, 1723-1728.

29. Furukawa Y, Yamabe M, Itoh A, and Inagaki T. (1982). "Emission Characteristics of Single-Crystal $LaB_6$ Cathodes with (100) and (110) Orientations," J. Vac. Sci. Technol., 20, 199-203.

30. Futamoto M, Hosoki S, and Kawabe U. (1979). "Field-Ion and Electron Microscopies of Carbon Tips," Surface Science, 86, 718-722.

31. Futamoto M, Yuito I, and Kawabe U. (1982). "Study of Titanium Carbide Field Emitters by Field-Ion Microscopy, Field-Electron Emission Microscopy, Auger Electron Spectroscopy and Atom Probe Field Ion Microscopy," Surface Science, 120, 90-102.

32. Gasser RPH, Gowan PM, and Newman DG. (1968). "The Chemisorption of Carbon Monoxide on Tantalum Monocarbide," Surface Science, 11, 317-326.

33. Gasser RPH, Gowan PM, and Newman DG. (1969). "The Chemisorption of Hydrogen on Tantalum Monocarbide," Surface Science, 14, 7-12.

34. Gesley MA, and Swanson LW. (1985). "Spectral Analysis of Adsorbate Induced Field Emission Flicker (1/f) Noise -- Canonical Ensemble," Phys. Rev. B, (in press).

35. Gomer R. (1973). "Current Fluctuations from Small Regions of Adsorbate Covered Field Emitters, A Method for Determining Diffusion Coefficients on Single Crystal Planes," Surface Science, 38, 373-393.

36. Hainfeld JF. (1977). "Understanding and Using Field Emission Sources," Scanning Electron Microsc., 1977: I: 591-604.

37. Hibino M, and Siegel BM. (1972). "Illuminating System for High Resolution Transmission Microscopy Using a Field Emission Source and Prefield of the Condenser-Objective," J. Appl. Phys., 43, (1972) pp 657-662.

38. Hosoki S, Yamamoto S, Futamoto M, and Fukuhara S. (1979). "Field Emission Characteristics of Carbon Tips," Surface Science, 86, 723-733.

39. Ishimaru H. (1984). "All Aluminum Alloy Ultrahigh Vacuum System for a Large-Scale Electron Positron Collider," J. Vac. Sci. Technol., A2, 1170-1175.

40. Ishimaru H. (1978). "Bakable Aluminum Vacuum Chamber and Bellows with an Aluminum Flange and Metal Seal for Ultrahigh Vacuum," J. Vac. Sci. Technol., 15, 1853-1854.

41. Kang NK, Orloff J, Swanson LW, and Tuggle D. (1981). "An Improved Method for Numerical Analysis of Point Electron and Ion Source Optics," J. Vac. Sci. Technol., 19, 1077-1081.

42. Kang NK, Tuggle D, and Swanson LW. (1983). "A Numerical Analysis of the Electric Field and Trajectories with and without the Effect of Space Charge for a Field Electron Source." Optik 63, 313-331.

43. Kawasaki K, Senzaki K, Kumashiro Y, and Okada A. (1977). "Energy Distribution of Field-Emitted Electrons from TiC Single Crystal," Surface Science, 62, 313-316.

44. Kelly J, Groves T and Kuo HP. (1981). "A High-Current, High Speed Electron Beam Lithography Column," J. Vac. Sci. Technol., 19, 936-940.

45. Komoda T, and Saito S. (1972). "Experimental Resolution Limit in the Secondary Electron Mode for a Field Emission Source Scanning Electron Microscope," Scanning Electron Microsc., 1972; 129-136.

46. Komoda T, Todokoro H, and Nomura S. (1977). "Single Atom Image Observation by Means of Scanning Transmission Electron Microscope," Hitachi Review, 26, No. 4, 151-156.

47. Latham RV, and Wilson DA. (1983). "The Energy Spectrum of Electrons Field Emitted from Carbon Fibre Micropoint Cathodes," J. Phys. D: Appl. Phys., 16, 455-463.

48. Lea C. (1973). "Field Emission from Carbon Fibres," J. Phys. D: Appl. Phys., 6, 1105-1114.

49. Martin EE, Trolan JK, and Dyke WP. (1960). "Stable, High Density Field Emission Cold Cathode," J. Appl. Phys., 31, 782-789.

50. Nagatani N, and Okura A. (1977). "Enhanced Secondary Electron Detection at Small Working Distance in the Field Emission SEM," Scanning Electron Microsc., 1977; I: 695-702.

51. Nomura S, Komoda T, Kamiryo T, and Nakaizumi Y. (1973). "Stable Field Emission Gun with an Electronic Feedback System," Scanning Electron Microsc., 1973; 65-72.

52. Orloff J. (1984). "A Comparison of Electron Guns for High Speed E-Beam Inspection," Scanning Electron Microsc., 1984; IV: 1585-1600.

53. Orloff J. (1984). "Thermal Field Emission for Low Voltage SEM," Bailey GW Ed, Proc. 42nd Annual Meeting of the Microscopy Society of America, San Francisco Press Inc., 450-453.

54. Orloff J and Swanson LW. (1979). "Asymmetric Electrostatic Lens for Field Emission Microprobe Applications," J. Appl. Phys., 50, 2494-2501.

55. Orloff J and Swanson LW. (1979). "A Study of Some Electrostatic Gun Lenses for Field Emission," Scanning Electron Microsc., 1979; I: 39-44.

56. Orloff J and Swanson LW. (1981). "Optical Column Design with Liquid Metal Ion Sources," J. Vac. Sci. Technol., 19, 1149-1152.

57. Orloff J and Swanson LW. (1982). "Some Considerations on the Design of a Field Emission Gun for a Shaped Spot Lithography System," Optik, 61, 237-245.

58. Oshima C, Tanaka T, and Aono M. (1979). "Small Changes in Work Function of the TiC (001) Surface with Chemisorption of $O_2$ and $H_2O$," Appl. Phys. Lett., 35, 822-823.

59. Oshima C, Aono M, Tanaka T, Kawai S, and Shibata Y. (1981). "Clean TiC(001) Surface and Oxygen Chemisorption Studied by Work Function Measurement, Angle-Resolved X-ray Photoelectron Spectroscopy, Ultraviolet Photoelectron Spectroscopy and Ion Scattering Spectroscopy," Surface Science, 102, 312-330.

60. Oshima C, Souda R, Aono M, and Ishizawa Y. (1983). "Stable Field Electron Emission from a Tungsten Tip under the Ultrahigh Vacuum of $10^{-10}$ Pa," Appl. Phys. Let., 43, 611-612.

61. Oshima C, Souda R, Otani S, and Ishizawa Y. (1984). "Stable TiC Field Emitter," Oyo Buturi, 53, 206-211 (in Japanese).

62. Ranc S, Pitaval M, and Fontaine G. (1976). "Stable Field Emission for Electron Beam Illumination," Surface Science, 57, 667-678.

63. Saitou N. (1977). "Trajectory Analysis of Ions Formed in the Field Emitter Inter Electrode Region," Surface Science, 66, 346-356.

64. Shimizu R, Kuroda K, Suzuki T, Nakamura S, Suganuma T, and Hashimoto H. (1973). "Field Emission Scanning Electron Microscope with Parallel Plate Gun Electrodes," Scanning Electron Microsc. 1973; 73-80.

65. Shrednik VN. (1961). "Investigation of Atomic Layers of Zirconium on the Faces of a Tungsten Crystal by Means of Electron Ion Projectors," Soviet Phys.-Solid State, 3, 1268-1279.

66. Smith R. (1984). "The Sputtering of Field Electron Emitters by Self-Generated Positive Ions," J. Phys. D: Appl. Phys., 17, 1045-1053.

67. Someya T, Goto T, Harada Y, Yamada K, Koide H, Kokubo Y, and Watanabe M. (1974). "On Development of a 100 kV Field Emission Electron Microscope," Optik, 41, 225-244.

68 Stille G and Astrand B. (1978). "A Field Emitter Electron Beam Exposure System," Physica Scripta, 18, 367-371.

69. Swann DJ and Smith KCA. (1973). "Life-Time and Noise Characteristics of Tungsten Field Emitter," Scanning Electron Microsc. 1973; 41-48.

70. Swann DJ and Kynaston D. (1973). "The Development of a Field Emission SEM," Scanning Electron Microsc. 1973; 57-64.

71. Swanson LW and Crouser LC. (1969). "Angular Confinement of Field Electron and Ion Emission," J. Appl. Phys., 40, 4741-4749.

72. Swanson LW. (1978). "Current Fluctuations from Various Crystal Faces of a Clean Tungsten Field Emitter," Surface Science, 70, 165-180.

73. Swanson LW and Tuggle D. (1981). "Recent Progress in Thermal Field Electron Source Performance," Appl. Surface Science, 8, 185-196.

74. Swanson LW and Bell AE. (1973). "Recent Advances in Field Electron Microscopy of Metals." Advances in Electronics and Electron Physics, 32, 193-309. (Academic Press)

75. Swanson LW and Martin NA. (1975). "Field Electron Cathode Stability Studies;Zirconium/Tungsten Thermal-Field Cathode," J. Appl. Phys., 46, 2029-2050.

76. Swanson LW. (1975). "Comparative Study of the Zirconiated and Built-up W Thermal Field Cathode," J. Vac. Sci. Technol., 12, 1228-1233.

77. Swanson LW, Tuggle D and Li J-Z. (1983). "The Role of Field Emission in Submicron Electron Beam Testing," Thin Solid Films, 106, 241-255.

78. Takigawa T, Sasaki I, Meguro T, and Motoyama K. (1982). "Emission Characteristics of Single Crystal $LaB_6$ Electron Gun," J. Appl. Phys., 53, 5891-5897.

79. Tamura N. (1979). "Basic Study of TF Emission," Scanning Electron Microsc. 1979; I: 31-38.

80. Todokoro H, Saitou N, and Yamamoto S. (1982). "Role of Ion Bombardment in Field Emission Current Instability," Japanese J. Appl. Phys., 21, 1513-1516.

81. Tonomura A. Matsuda T, Endo J, Todokoro H, and Komoda T. (1979). "Development of a Field Emission Electron Microscope," J. Electron Microsc., 28, 1-11.

82. Tuggle D, Swanson LW, and Orloff J. (1979). "Application of a Thermal Field Emission Source for High Resolution, High Current E-Beam Microprobes," J. Vac. Sci. Technol., 16, 1699-1703.

83. Tuggle DW and Watson SG. (1984). "A Low Voltage Field Emission Column with a Schottky Emitter," G.W. Bailey, Ed., Proc. 42nd

Annual Meeting of Electron Microscopy Society of America, San Francisco Press, Inc. 454-457.

84. Veneklasen LH and Siegel BM. (1972). "Oxygen Processed Field Emission Source," J. Appl. Phys., 43, 1600-1604.

85. Veneklasen LH and Siegel BM. (1972). "A Field-Emission Illumination System Using a New Optical Configuration," J. Appl. Phys., 43, 4989-4996.

86. Vogel SF. (1970). "Pyrolytic Graphite in the Design of a Compact Inert Heater of a Lanthanum Hexaboride Cathode," Rev. Sci. Instrum., 41, 585-587.

87. Wardly GA. (1973). "Potential of Field Emission Cathodes for Microfabrication," J. Vac. Sci. Technol., 10, 975-978.

88. Weisner JC. (1973). "Characteristics and Application of Pointed Cathodes in Scanning Electron Microscopes," Scanning Electron Microsc., 1973; 33-40.

89. Wiggins JW. (1977). "Practical Considerations for STEM Optics," Scanning Electron Microsc. 1977; I: 673-682.

90. Wolfe JE. (1979). "Operational Experience with Zirconiated TF Emitters," J. Vac. Sci. Technol., 16, 1704-1708.

91. Yamamoto S, Hosoki S, Fukuhara S, and Futamoto M. (1979). "Stability of Carbon Field Emission Current," Surface Science, 86, 734-742.

92. Zaima S, Sase M, Adachi H, and Shibata Y. (1978). "Measurements of Energy Spread of Thermal Field Emitted Electron Flow from Tungsten," J. Phys. D: Appl. Phys., 11, L179-L180.

93. Zaima S, Saito K, Adachi H, Shibata Y, Hojo H, and Ono M. (1980). "Field Emission from TaC," Yashiro and Igata, Ed., 27th Int. Field Emission Symposium, Tokyo. Maruzen. 348-357.

94. Zaima S, Sase M, Adachi H, Shibata Y, Oshima C, Tanaka T, and Kawai S. (1980). "Spread of Total Energy Distribution of Thermal Field Emitted Electrons from $LaB_6$ Single Crystal Needles," J. Phys. D: Appl. Phys., 13, L47-L49.

95. Zaima S, Oshima C, Otani S, Aono M, Adachi H, and Shibata Y. (1981). "Change in Work Function of $TiC_x$ Single Crystal with Oxygen Chemisorption," Swanson and Bell, Ed., 28th Int. Field Emission Symposium, Oregon. Oregon Graduate Center. 156-159.

96. Zaima S, Adachi H, and Shibata Y. (1984). "Promising Cathode Materials for High Brightness Electron Beams," J. Vac. Sci. Technol., B2, 73-78.

## Discussion with Reviewers

A.V. Crewe: One of the most important characteristics of a field emission source is its small source size. Yet no values, experimental or theoretical, are given anywhere in this paper. Yet if this size were not in the range of Å it would have no value at all. For example, while treatment with Zr reduces the total angle of emission, what does it do to the source size?
Author: It is true that in the view of the electron optics the source size of an electron source is an important factor, but it is set outside of this review paper, thus no values are given in the text. In a typical case of cold field emission the electron optical source size is about 50 Å, while in the case of thermal field emission source it is about 150 Å [52]. A comparison of electron guns of cold field emission and thermal field emission for high speed electron beam inspection has been given by J. Orloff [52], which gives useful information about the features of both types of field emission guns.

The reduction of the total angle of emission from the ZrO/W(100) cathode occurs due to the flat apex surface created by the facetting of (100) face of the W crystal. This effect makes about a 60% increase in the virtual source size compared with the case of a round apex. A detailed discussion of this aspect can be found in text ref. 42 and Swanson, 1984 (Swanson LW. (1984). "Field Emission Source Optics," in: Electron Optical Systems, (eds.) J.J. Hren, F.A. Lenz, E. Munro, P.B. Sewell, SEM, Inc., AMF O'Hare, IL 137-147).

A.V. Crewe: Energy spread of the electrons is also important but is not given very much attention. In spite of the flat statements given in the text: "The energy spread...emission...." it appears that the only data is theoretical (Fig. 13). In any case, it only applies to two types of source.
Author: The electron energy distribution is also important as the reviewer points out when considering the chromatic aberration of the electron optical system, but detailed discussion of this aspect has been set outside of this review paper. The electron energy distribution is considered in so far as it is one of the characteristic features of the field emission mechanism. The theoretical data given in Fig. 13 were calculated under the assumption that the electrons in the metal obey the free electron model and that the transmission coefficient of electrons through the surface barrier can be determined by the WKB approximation. These calculated results are in good agreement with the experimental results both in the cases of W [92] and $LaB_6$ [94]. The Fermi energy has a value of several eV for suitable field emission cathode materials, so that it has almost no effect on the calculated energy spread. Only the work function has an effect on

the field emission energy distribution. Therefore the same curve can be applied to materials with similar work function values, e.g. the $LaB_6$ and ZrO/W(100) cathodes, since the latter has a work function of about 2.7 eV.
When the emission current density is high, the energy spread increases due to Coulomb interaction of the electrons. Detailed discussion of this aspect and some experimental results can be found in reference [10].

K.C.A. Smith: Does the choice of anode material affect ion production and thus the stability of the emission current in any way? If so, what is the best material?

Author: Most of the molecules and ions from the anode are created by electron stimulated desorption (ESD) of the adsorbed gas molecules due to electron bombardment at the anode surface. The number of neutral gas molecules is about two orders higher than that of the ionized molecules. The neutral molecules also decrease the current stability by increasing the pressure of the vacuum. Thus materials which have a low capacity for chemisorption by residual gas molecules are desirable. However, there is apparently no experimental report that has yet been published on this topic.

K.C.A. Smith: Does operation of the anode at an elevated temperature result in an improvement of the stability of emission?

Author: Theoretically, yes, because the amount of adsorbed gas is small at high temperatures. However no systematic experimental report has been published so far, within this author's knowledge. In the cases of the stable cold field emission from W reported by Oshima et al [60] and Dyke et al [49] the anode materials were molybdenum or tungsten. The anodes were heated to temperatures on the order of 2000C before operation for the purpose of degassing, although during operation they were at or below room temperature. In the case of the stable cold field emission from TiC reported by Adachi et al [2], the anode material was a non-magnetic stainless steel coated with a phosphorescent material.

K.C.A. Smith: Please explain what is meant by the "threshold temperature for current fluctuation of W".

Author: The threshold temperature is typically where the relative rms current fluctuation becomes greater than 0.1%.

K.C.A. Smith: The few practical and successful commercial electron optical systems employing cold field W emitters have all depended on the achievement of a very high vacuum with attendant high cost. What are the prospects of employing the carbides or other new materials to realize commercial systems of lower cost and greater flexibility and ease of use?

Author: The ZrO/W(100) thermal field emission source can be operated in a vacuum of $10^{-8}$ Torr ($1.3 \times 10^{-6}$ Pa) [76]. This vacuum requirement is about three orders of magnitude less than that required for stable cold field emission from W as reported by Oshima et al [60]. While cold field emission from a TiC single crystal was obtained in a vacuum of $2.7 \times 10^{-8}$ Pa, as shown in Fig. 8, further reduction of the vacuum requirement could be possible if it is operated in a thermal field emission mode.

D.C. Joy: I am still not sure that I understand why different crystal faces, and different materials, show such different noise spectra. Is this simply due to different atomic mobilities on these faces, or is there a more fundamental explanation (i.e. a quantum mechanical effect)?

Author: Field emission currents from a W field emitter still exhibits 1/f noise even if it is operated in an extremely low residual gas pressure of $10^{-10}$ Pa [60], which is attributed to surface atom migration. The current fluctuation measurements from different crystal orientations reported by Swanson [72] were also done in an extremely low residual gas pressure of less than $5 \times 10^{-10}$ Torr ($6.7 \times 10^{-8}$ Pa), which was performed by immerging the whole vacuum system in a liquid nitrogen bath. In this case, the different noise spectra are caused by the different atomic mobilities on the various crystal surfaces. But such low residual gas pressures are not the case for a practical field emission electron source. Thus in practical cases the current fluctuations are expected to be caused mainly by residual gas interactions with the cathode surface. The adsorption and the desorption process and the movement of the adsorbed gas molecules on the crystal surface cause the current fluctuations. The adsorbed gas molecules change the work function and hence the emission current. The bombardment of the residual gas ions stimulates desorption of the adsorbed gas, and thus the current fluctuation depends on both the emission current level and the residual gas pressure, as shown in Figure 4. These two factors are directly related to the rate of ion creation. Therefore variations in residual gas sticking probabilities and surface diffusivities cause the work function fluctuations, which in turn produce the observed orientation dependent current fluctuations. This author believes that the lack of 1/f noise in the field emission current from TiC is caused by its low level of gas adsorption, which therefore causes little change in the work function.
In the case of the 1/f noise in the ZrO/W(100) thermal field emitter can be expected due to the surface migration of the atoms at the cathode surface due to the high operating temperature. The evidences for the atomic motions are the facetting of (100) face and a movement of a ring structure in the emission patterns observed during operation.

J.R.A. Cleaver: Please indicate what etching procedures and electrolytes have been developed for the transition metal carbide emitters. Can the etching be controlled to yield the necessary apex radius? What, if any, is the influence of flashing on the tip profile, surface finish, and apex radius?

Author: The etching process was fundamentally the same as that for the W field emitter except for the electrolytes used. Almost the same level of reproducibility was obtained. The etching solution of 20% HF in $H_2SO_4$ can be used. The flashing induced some facetting at the tip of the cathode, which did affect the emission patterns.